Simulation Analysis of the Binding Interactions in the RNase A/3'-UMP Enzyme-Product Complex as a Function of pH

3 AUTHORS, INCLUDING:

Carmay Lim
Academia Sinica
144 PUBLICATIONS **4,082** CITATIONS

Simulation Analysis of the Binding Interactions in the RNase A/3′-UMP Enzyme–Product Complex as a Function of pH[†]

John E. Straub,[‡] Carmay Lim,[§] and Martin Karplus*

Contribution from the Department of Chemistry, Harvard University, 12 Oxford Street, Cambridge, Massachusetts 02138

Received September 18, 1992. Revised Manuscript Received September 27, 1993[⊕]

Abstract: Stochastic boundary simulations are performed to study the binding of 3′-uridine monophosphate to bovine pancreatic ribonuclease A for three protonation states of the enzyme–product complex. Because charged species are involved, the structure of the enzyme–product complex provides a sensitive test of the method used for treating the long-range electrostatic interactions. To avoid spurious effects resulting from group-switch or atom-switch electrostatic potential truncation schemes, an extended electrostatics algorithm is used. It allows for the inclusion of all electrostatic interactions through a pairwise charge–charge interaction at short distances and charge–group multipole moment interactions at large separations. Since X-ray data are available only at low pH where the phosphate was assumed to be monoanionic, the present simulations provide predictions concerning the structure and interactions of the enzyme–product complex at other pH values. In particular, the role of specific residues in the binding of the product is examined. Maximal binding is found to occur when a phosphate dianion interacts with positively charged His 12 and 119; a fall in binding is expected at low and neutral pH due mainly to the loss of enzyme interactions with the phosphate and base. All three groups of the product (the base, ribose, and phosphate) are involved in binding to the enzyme; Thr 45, Lys 41, and a positively charged histidine (His 12 or His 119) are the respective recognition residues.

I. Introduction

A full understanding of ribonuclease A (RNase A) requires not only a description of its catalytic function but also a knowledge of the protein–nucleic acid interactions which determine its specificity. There have been numerous experimental studies of the binding of substrates and inhibitors to RNase A.[1] The positively charged active site of RNase A facilitates the binding of the substrate but binds the product more strongly[2] since the latter is a dianionic phosphate monoester whereas the substrate is a monoanionic diester. For example, at an ionic strength of 0.2 M, the dissociation constant of the product, 3′-uridine monophosphate (3′-UMP), is 0.05 mM at pH 5.5, 25 °C, which is an order of magnitude less than that of the substrate, cyclic-UMP (0.5 mM at pH 5.8, 27 °C). In this paper, we focus on the binding of the product, 3′-UMP, to RNase A, identify the key enzyme–mononucleotide interactions, and examine how these interactions change as a function of pH.

The 1.9-Å resolution X-ray structure of RNase A cocrystallized with 3′-UMP has been determined at pH 5.5.[3] At this pH, it was assumed that the two active site histidines, His 12 and His 119, are protonated and the phosphate is in the singly charged state (see below). There are two hydrogen bonds between O^2 and N^3 of the base and N and $O^{\gamma 1}$ of Thr 45, respectively, two hydrogen bonds from $O^{2'}$ of the sugar to His 12($N^{\epsilon 2}$) and Lys 41(N^ζ), and four hydrogen bonds from the phosphate oxygens to His 12, His 119, Phe 120, and Gln 11 (see Figure 1). Both proton[4] and ^{31}P NMR[5] solution studies support the X-ray results, since they
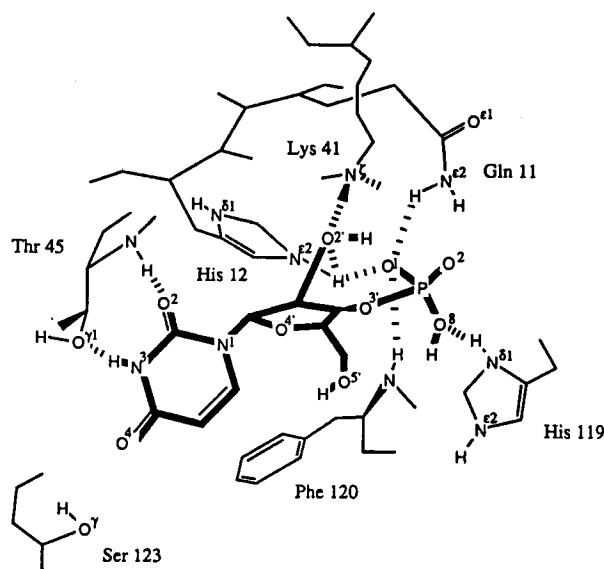
Figure 1. Schematic diagram of important hydrogen-bonding contacts between the key residues of the enzyme active site and the product (bold lines) in the X-ray structure.[3]

indicate that a doubly protonated His 12 interacts directly with the phosphate in the enzyme–product complex.

Ionization constants of the phosphate, His 12, and His 119 for the RNase A/3′-UMP complex have been determined from the pH dependence of proton and ^{31}P NMR chemical shifts, as shown in Table 1. The NMR data are compatible with the assumption that the observed maximum in the binding at pH 5.5 (Table 2) corresponds to the interaction between the phosphate dianion and the two protonated active site histidines. The fall in binding at lower pH (pH < 5.5) is presumed to be due to protonation of the phosphate group, whereas the fall in binding at higher pH (pH > 5.5) is due to deprotonation of His 12 and His 119. We examine this hypothesis by performing molecular dynamics simulations on the RNase A/3′-UMP complex in 3 different protonation states, viz., (i) with monoanionic 3′-UMP and protonated His 12 and His 119 (pH 4.0–4.5), (ii) with dianionic

(1) Richards, F. M.; Wyckoff, H. W. *The Enzymes* **1971**, *4*, 647.
(2) Brünger, A. T.; Brooks, C. L., III; Karplus, M. *Proc. Natl. Acad. Sci. U.S.A.* **1985**, *82*, 8458.
(3) Gilbert, W. A.; Fink, A. L.; Petsko, G. A., unpublished (the coordinates are available from G. A. Petsko, Brandeis University).
(4) Meadows, D. H.; Roberts, G. C. K.; Jardetsky, O. *J. Mol. Biol.* **1969**, *45*, 491.
(5) Gorenstein, D. G.; Wyrwicz, A. M.; Bode, J. *J. Am. Chem. Soc.* **1976**, *98*, 2308.

2592 *J. Am. Chem. Soc., Vol. 116, No. 6, 1994*

Straub et al.

Table 1. Ionization Constants

	pK_a		
molecule	His 12	His 119	phosphate[a]
RNase A/3'-UMP		7.5[b]	4.1[b]
RNase A/3'-UMP	6.5 ± 0.4[c]		4.6 ± 0.7[c]
RNase A/3'-UMP	6.2[d]	8.0[d]	
3'-UMP			5.8[b]
			5.9[c]
RNase A	5.8–6.0[e]	6.2–6.3[e]	

[a] $RPO_4^-H \rightarrow RPO_4^{2-} + H^+$. [b] From ^{1}H NMR;[24] base C5 and C6 proton chemical shift as a $f(pH)$ at 23 °C. Concentrations: RNase A, 0.0030 M; 3'-UMP, 0.0015 M; NaCl, 0.3 M. [c] From ^{31}P NMR;[5] chemical shift as a $f(pH)$ at 24 °C. Concentrations: RNase A, 0.0060M; 3'-UMP, 0.0060 M; ammonium formate, 0.1 M. [d] From ^{1}H NMR;[25] histidine C2-proton chemical shift as a $f(pH)$ (NB. Temperature not given in paper). Concentrations: RNase A, 0.0100 M; 3'-UMP, 0.012 M; NaCl, 0.2 M. [e] From ^{1}H NMR.[26]

Table 2. Association Constants for 3'-UMP/RNase A Binding as a Function of pH at 25 °C and 0.1 M KCl[27]

pH	$K/1000$ (M^{-1})	pH	$K/1000$ (M^{-1})
4.5	3.9	6.0	12.2
5.0	9.0	6.5	6.1
5.5	14.2	7.0	2.3

3'-UMP and protonated His 12 and His 119 (pH $\approx$ 5.5), and (iii) with dianionic 3'-UMP, neutral His 12, and protonated His 119 (pH $\approx$ 6.5). We refer to these three protonation states of the RNase A/3'-UMP complex as the low, optimal, and neutral pH states. The present simulations provide information concerning the groups involved (on the enzyme and on the product) and how their interactions change with pH. The important role of solvent is also made clear. The simulation studies are of particular interest because X-ray results are available only at low pH, where the phosphate is monoanionic and the two histidines are protonated.

In section II, we describe the methods used in the simulations. The dominant interactions between the product and the enzyme are electrostatic. Preliminary calculations showed that group-switch truncation of these long range forces with cutoff distances less than 12 Å leads to dissociation of the product, while simulations with no potential truncation result in a stable bound state of the enzyme–product complex. To approximate the no-cutoff calculation, we use the extended electrostatics method.[6] We compare the results with those from an atom-based truncation scheme. These results are presented in section III. Also in section III, we analyze the simulation results for the three protonation states of the RNase A/3'-UMP complex. The conclusions are summarized in section IV. The Appendix contains a brief discussion of the nature of the force convergence (in magnitude and direction) for four commonly used truncation schemes for the nonbonded interactions.

II. Methodology

The active site of RNase A has a positive charge of 8 e at physiological pH (pH $\approx$ 6–7). Since the interaction of the positively charged active site histidines with the phosphate group of the product is predominantly electrostatic, this system provides a very sensitive probe of the effects of the truncation used for the long-range electrostatics interactions. In this section we briefly describe the system and outline the methods employed in the simulations, the details of the treatment of the Coulombic interactions, and the parameters of the force field.

A. System. The starting point for the simulations was the 1.9-Å resolution X-ray structure of RNase A/3'-UMP.[3] Since we are primarily interested in the structure of the active site where the product is bound, we initially chose to study a reduced system which included only residues with one or more atoms that were within 16 Å of the phosphorous atom. To test whether this choice is satisfactory, we examined the electrostatic potential generated by the portion of the enzyme not included in the reduced system and its interaction energy with the product bound to the

active site. The X-ray structure of the RNase A/3'-UMP complex without the product and crystallographic water molecules was used to calculate the electrostatic potentials of the full and reduced enzyme by solution of the Poisson equation with a dielectric constant that changed from an internal dielectric constant of 4 to the solvent dielectric constant of 80 at the dielectric boundary;[7,8] the ionic strength was taken to be zero. The version 19 parameters for the CHARMM van der Waals radii and charges were employed.[9] Contour plots of the electrostatic potential for the reduced enzyme at radial distances greater than 10 Å from the phosphorus differed significantly from those of the full enzyme molecule. We found that Lys 1, Asp 14, and Arg 85, whose C^α–P distances are 16.9, 15.21, and 14.44 Å, respectively, had to be included to reproduce the full enzyme potential (within 0.25 kcal/mol) out to 12.5 Å from the phosphorus atom. The final reduced system was composed of 90 amino acid residues with the following connectivity: 1–14; 22; 25–27; 29–36; 39–49; 51; 53–54; 56; 58–60; 63; 65–69; 71–72; 75; 77–79; 81–85; 88–95; 104–114; and 116–124.

Stochastic boundary dynamics[2,10] was carried out on both the full and the reduced system (see below) to reduce the computation and to incorporate solvent in the active site region. A fully solvated protein represents a large number of atoms to be simulated. Often, a restricted region of the protein, such as the active site, is of particular interest. The stochastic boundary approximation provides a means of reducing the computational effort required by replacing much of the bulk solvent and protein far from the active site region by a static boundary potential of mean force and interaction with a heat bath. Atoms within an inner *active site region* are simulated explicitly according to Newton's equations of motion. Atoms in an intermediate *buffer region* are coupled to a heat bath and feel an external boundary potential which represents the solvent or protein not explicitly included in the simulation. Finally, some atoms are included but fixed in an outer *reservoir region*. Within the stochastic boundary approximation it is possible to provide an accurate representation of the system while greatly reducing the computational burden.[2,10]

In this work, the center of the system was chosen to be the phosphorous atom. Using the stochastic boundary approximation, protein and solvent atoms within 12 Å of the center (active site region) were propagated according to Newton's equations using the Verlet algorithm and a time step of 1 fs. Non-hydrogen protein and solvent atoms in the volume outside 12 Å and inside 16 Å (buffer region) are assumed to be in direct contact with a heat bath and were propagated according to the Langevin equation with harmonic constraints determined from averaged X-ray temperature factors. The averaged X-ray temperature factors ($B = (^8/_3)\pi^2 < \Delta R^2 >$) employed were 14 Å^2 for backbone, C^α, and side-chain atoms, 15 Å^2 for β position atoms, 16 Å^2 for γ position atoms, and 17 Å^2 for all other atoms. The heat bath temperature used was 300 K, and the friction constant for protein and water atoms was 62 ps^{-1}. The constraining force and friction constants for the protein atoms were scaled using a cubic spline function which ranged from zero at 12 Å to a maximum of one-half at 14 Å. Atoms outside 16 Å (reservoir region) were held fixed (but they contribute to the forces on moving atoms). All bonds to hydrogen atoms were constrained to have fixed length and were propagated using the SHAKE algorithm.[11] Solvent molecules, represented by a modified TIP3P potential,[12] were constrained relative to the center of the system by a constraining potential (of the Lennard-Jones form) at 16 Å; they were treated by molecular dynamics in the active site region and Langevin dynamics in the buffer region.

The forces on the atoms and their dynamics were calculated with the CHARMM program.[9] Initially, to relieve strains in the X-ray structure, the system was minimized with weak constraints on the protein atoms for 100 steps using the Powell algorithm.[13] Next a 18.5-Å sphere of equilibrated TIP3P water was centered on the phosphorous atom in the X-ray structure. All solvent atoms within 2.6 Å of a heavy atom and outside 16 Å of the phosphorus atom were removed; to mimic the bulk water in contact with the active site region of the protein, 171 water molecules were added to the 41 crystal waters. The remaining solvent was minimized for 100 steps to relieve close contacts and equilibrated

(6) Stote, R. H.; States, D. J.; Karplus, M. *J. Chim. Phys.* **1991**, *88*, 2419.

(7) Bashford, D.; Karplus, M. *Biochemistry* **1990**, *29*, 10219.

(8) Lim, C.; Bashford, D.; Karplus, M. *J. Phys. Chem.* **1991**, *95*, 5610.

(9) Brooks, B. R.; Bruccoleri, R. E.; Olafson, B. D.; States, D. J.; Swaminathan, S.; Karplus, M. *J. Comput. Chem.* **1983**, *4*, 187.

(10) Brooks, C. L., III; Karplus, M. *J. Chem. Phys.* **1983**, *79*, 6312.

(11) van Gunsteren, W. F.; Berendsen, H. J. C. *Mol. Phys.* **1977**, *34*, 1311.

(12) Jorgensen, W. L.; Chandrasekhar, J.; Madura, J. D.; Impey, R. W.; Klein, M. L. *J. Chem. Phys.* **1983**, *79*, 926.

(13) Press, W. H.; Flannery, B. P.; Teukolsky, S. A.; Vetterling, W. T. *Numerical Recipes: The Art of Scientific Computing*; Cambridge University Press: Cambridge, 1986.

with 4 ps of Langevin dynamics. The solvent overlay was repeated, which resulted in the addition of 20 water molecules; this was followed by 4 ps of Langevin dynamics on the solvated complex. A third solvent configuration was overlaid, adding 11 water molecules, followed by minimization to obtain the final system with 243 water molecules. Langevin dynamics on the entire solvated system was performed for a 10-ps equilibration phase. This was followed by 20–25 ps of molecular dynamics for the part of the system in the active site region and Langevin dynamics for the part of the system within the buffer region; the rest of the system (protein outside 16 Å) was kept fixed.

B. Group Definitions for Nonbonded Interactions. We simulated the enzyme–product system using two different treatments of the electrostatic interactions. The first (referred to as extended electrostatics or EE) uses the extended electrostatics method[6,9] to treat the long-range electrostatic interactions. Atom pairs within a prescribed cutoff distance ($r_c = 12$ Å) interact according to the full pairwise potential that includes both van der Waals and electrostatic contributions; atom pairs outside are assumed to interact through electrostatic forces alone, and they are approximated by a multipole expansion up to the quadrupolar term.

The total electrostatic potential at a point $\vec{r}_i$ can be written as a sum of short- and long-range interactions:[6]

$$\Phi_{\text{total}}(\vec{r}_i) = \Phi_{\text{near}}(\vec{r}_i) + \Phi_{\text{ext}}(\vec{r}_i) \tag{1}$$

The short-range contribution to the electrostatic potential $\Phi_{\text{near}}(\vec{r}_i)$ is a sum of pairwise contributions of all charges q_j at $\vec{r}_j$ where $|\vec{r}_i - \vec{r}_j| \leq r_c$:

$$\Phi_{\text{near}}(\vec{r}_i) = \sum_{j \neq i} \frac{q_j}{\epsilon |\vec{r}_i - \vec{r}_j|} \tag{2}$$

ϵ is the dielectric constant taken to be unity in this work.

The long-range contribution to the electrostatic potential $\Phi_{\text{ext}}(\vec{r}_i)$ may be ignored (set to zero by truncating the potential after r_c) or treated exactly by setting $r_c = \infty$. However, the latter "no-cutoff" method represents a prohibitively large computational overhead for most systems. The extended electrostatics method provides an accurate means of approximating the long-range contribution to the electrostatic potential.[6] Atoms are partitioned into "groups" which are typically electroneutral. The long-range contribution to the electrostatic potential $\Phi_{\text{ext}}(\vec{r}_i)$ represents the contribution to the total electrostatic potential of all charges forming groups whose center is a distance greater than the cutoff distance r_c from $\vec{r}_i$. The electrostatic potential at $\vec{r}_i$ due to a group of atoms centered outside the cutoff distance is then approximated by a multipole expansion which includes the group charge, group dipole, and group quadrupole.

The extended electrostatic energy for a given configuration is

$$E_{\text{ext}} = \sum_i q_i \Phi_{\text{ext}}(\vec{r}_i) \tag{3}$$

The force acting on a charge q_i at $\vec{r}_i$ due to interaction with the extended electrostatic potential is

$$\vec{F}_{\text{ext}} = q_i \vec{\nabla} \Phi_{\text{ext}}(\vec{r}_i) \tag{4}$$

The extended electrostatic forces were updated every 10 integration steps. Between updates the potential was approximated by a linear interpolation from the position of the ith atom at the time of update, $\vec{r}_{i0}$, to the current position, $\vec{r}_i$, as

$$\Phi_{\text{ext}}(\vec{r}_i) \approx \Phi_{\text{ext}}(\vec{r}_{i0}) + (\vec{r}_i - \vec{r}_{i0}) \vec{\nabla} \Phi_{\text{ext}}(\vec{r}_{i0}) \tag{5}$$

An abrupt cutoff at 12 Å was used to truncate the van der Waals potential.

The second potential truncation method (referred to as atom-switch or ASW) uses the atom-switch method to truncate the van der Waals potential and the long-range electrostatic forces, i.e., the pair potential is multiplied by the switching function

$$S(r) = \begin{cases} 1 & r \leq r_{\text{on}} \\ \left[\dfrac{(r_{\text{off}}^2 - r^2)^2 (r_{\text{off}}^2 - 3r_{\text{on}}^2 + 2r^2)}{(r_{\text{off}}^2 - r_{\text{on}}^2)^3} \right] & r_{\text{on}} < r \leq r_{\text{off}} \\ 0 & r > r_{\text{off}} \end{cases} \tag{6}$$

where $r_{\text{off}} = 12$ Å and $r_{\text{on}} = 8$ Å.

Table 3. Summary of Nonbonded Parameters for Histidine

atom	ϵ (kcal/mol)	$r_{\text{min}}/2$ (Å)	charge His+	charge His0
C_β	0.1142	2.235	0.10	0.00
C_γ	0.12	2.1	0.15	−0.08
$N_{\delta 1}$	0.2384	1.6	−0.30	−0.29
$C_{\delta 2}$	0.12	2.1	0.20	0.27
$C_{\epsilon 1}$	0.12	2.1	0.45	0.32
$N_{\epsilon 2}$	0.12	2.1	−0.30	−0.50
$H_{\delta 1}$	0.0498	0.8	0.35	0.28
$H_{\epsilon 2}$	0.0498	0.8	0.35	

In each of the above systems we employed the stochastic boundary approximation (see above), but the number of atoms included in each system is different. The EE system includes the entire enzyme–product system consisting of 1195 protein atoms (124 amino acid residues), 24 product atoms, and 243 water molecules. The ASW system includes only the amino acids which are in the stochastic boundary region (as described above), since we are primarily interested in the structure of the active site where the product is bound.

In the extended electrostatics method, an atom A which is outside a certain distance from another atom B will interact with the total charge, dipole, and quadrupole of a group of atoms containing atom B. Atoms in each residue of the CHARMM potential are divided into groups, comprised typically of two or three atoms, which are electroneutral or have integral charge. For the full RNase system there are 12 groups with no charge, 645 neutral groups, and 65 charged groups. The phosphate was treated as a group (O[3'], P, O[1P], O[2P], O[8], H[8]); the sugar was defined as three groups, (H[5'], O[5'], C[5']), (C[4'], O[4'], C[1']), and (C[2'], O[2'], H[2'], C[3']); and the base was divided into three electroneutral groups (N[1], C[2], O[2]), (N[3], H[3], C[4], O[4]), and (C[5], C[6]) (see below).

C. Parameters. All calculations employed the CHARMM force field using the version 19 parameter set in which polar hydrogens are treated explicitly and nonpolar hydrogens are treated in the extended atom representation. Exceptions are the parameters for the neutral histidine residues and the 3′-uridine monophosphate product; their charges and Lennard-Jones parameters are listed in Tables 3 and 4.

The phosphate charges were derived as follows. Monoanionic and dianionic 2′-hydroxyethyl phosphate, modeling the monoanionic and dianionic product, respectively, had been fully optimized at the HF/3-21G* level. Atomic charges were derived from a fit of a partial charge model to the *ab initio* electrostatic potentials using the CHELP program.[14] Such fitted charges are known to lead to an overestimation of interaction energies with water molecules[15] and were thus scaled by 0.75 (appropriate for the HF/3-21G* basis set). Following the scaling, the total charge of the molecule is no longer integral. To correct this, a small amount of charge (equal to the difference between the integral charge minus the total charge after scaling) was distributed across all atoms, in proportion to their absolute charge, to recover the total charge of the molecule and rounded to the nearest tenth of a unit charge to give the final values listed in Table 4. The charges for the monoanionic phosphate are in close agreement with those used in molecular dynamics simulations of the RNase A complexes[2,16] (Table 4); the latter were originally derived from molecular orbital calculations by Liebmann *et al.*[17] The dianionic phosphate charges are in good agreement with X-ray refined charges determined from a 0.77-Å resolution X-ray structure of disodium guanosine 5′-monophosphate heptahydrate.[18]

The uracil parameters were derived in a similar manner. The electrostatic potential was calculated from HF/6-31G wave functions of the base and fitted to an atomic point charge model using the CHELP program. The charges assigned to the nonpolar hydrogens were then combined with the associated heavy atom charge to arrive at the polar hydrogen potential model. The resulting charges were scaled by 0.737 (appropriate for the HF/6-31G basis set) and then rounded to give the final charges in Table 4.

(14) Chirlian, L. E.; Francl, M. M. *J. Comput. Chem.* **1987**, *8*, 894.

(15) Reiher, W. Ph.D. Thesis, Harvard University, Cambridge, MA, 1986. The parameters are available in the CHARMm program (ref 9) that can be obtained from Harvard University by writing to the senior author.

(16) Haydock, K.; Lim, C.; Brünger, A.; Karplus, M. *J. Am. Chem. Soc.* **1990**, *112*, 3826.

(17) Liebmann, P.; Loew, G.; Mclean, A. D.; Pack, G. R. *J. Am. Chem. Soc.* **1982**, *104*, 691.

(18) Pearlman, D. A.; Pandit, J.; Kim, S.-H. *Acta Crystallogr.* **1990**, *B42*, 379.

2594 *J. Am. Chem. Soc., Vol. 116, No. 6, 1994*

Straub et al.

Table 4. Summary of Nonbonded Parameters for 3'-Uridine Monophosphate

atom	ε (kcal/mol)	$r_{min}/2$ (Å)	charge UMP-	UMP2-
			Phosphate	
O3'	0.1204	1.6	-0.55 (-0.46)[a]	-0.60 (-0.58)[b]
P	0.12	2.1	1.30 (1.36)[a]	1.30 (1.27)[b]
O1P	0.1204	1.6	-0.70 (-0.72)[a]	-0.90 (-0.89)[b]
O2P	0.1204	1.6	-0.70 (-0.72)[a]	-0.90 (-0.97)[b]
O3P	0.1204	1.6	-0.70 (-0.71)[a]	-0.90 (-1.07)[b]
H	0.0498	0.8	0.35 (0.25)[a]	
			Uracil	
N1	0.16	1.75	-0.14 (-0.57)[c]	
C2	0.09	1.8504	0.69 (0.90)[c]	
O2	0.2304	1.6	-0.55 (-0.49)[c]	
N3	0.16	1.75	-0.52 (-0.76)[c]	
C4	0.09	1.8504	0.77 (0.57)[c]	
O4	0.2304	1.6	-0.55 (-0.39)[c]	
C5	0.12	2.1	-0.24 (-0.20)[c]	
C6	0.12	2.1	0.24 (0.37)[c]	
H3	0.0045	1.0	0.30 (0.35)[c]	
			Ribose	
C1'	0.0486	2.365	0.20	
C2'	0.0486	2.365	0.20	
O2'	0.1591	1.6	-0.60	
C3'	0.0486	2.365	0.00	
C4'	0.0486	2.365	0.20	
O4'	0.1204	1.6	-0.40	
C5'	0.1142	2.235	0.18	
O5'	0.1591	1.6	-0.48	
H2'	0.0498	0.8	0.40	
H5'	0.0498	0.8	0.30	

[a] Phosphate charges used in previous simulations of RNase A complexes.[2,16] [b] In parentheses are X-ray refined charges.[18] [c] In parentheses are AMBER charges.[28]

III. Simulation Results as a Function of pH

We simulated the enzyme–product complex for three different protonation states of His 12 and the product phosphate. A study of these protonation states provides first-order approximations to the effect of pH on the enzyme–product system. In accord with the results in Table 1 for the RNase A/3'-UMP complex, we assume that at low pH (2–4) His 12 is charged and the product is monoanionic, at optimal pH (5.5) His 12 is charged and the product is dianionic, and at neutral pH (≈ 7) His 12 is neutral and the product is dianionic; higher pH values at which other histidine residues (e.g., His 119) are neutral were not considered. The results of the simulations for the three pH values are presented below. We focus on the average structures obtained from the various simulations. We first describe the results obtained with the extended electrostatic model and their implications for product binding and then compare them with those obtained with the atom-switch model.

The data in Table 5 summarize the key hydrogen bonds that bind the product for the three (low, optimal, and neutral pH) protonation states; the corresponding atom-switch results are given in Table 6 and are discussed below. The important enzyme–product and solvent–product contacts are depicted in Figure 2 for the extended electrostatics simulations at (a) low, (b) optimal, and (c) neutral pH; a schematic drawing of these interactions at optimal pH is given in Figure 3. We list the number of solvent molecules in square brackets next to the number of hydrogen-bonding contacts. The number of molecules is always less than or equal to the number of bonding contacts. A large difference between the two indicates that there are bifurcated hydrogen bonds and strongly bound (less mobile) solvent molecules.

The total number of product–enzyme (product–solvent) interactions predicted by the extended electrostatics method is 6 (3), 8 (9), and 6 (9) for the low, optimal, and neutral pH states of the RNase A/3'-UMP complex, respectively (Table 5). This is in accord with the observation of maximal binding at pH 5.5,

Table 5. 3'-UMP Product Interactions with Enzyme and Solvent as a Function of pH Using the Extended Electrostatics Method[a]

	His 12+, 3'-UMP-	His 12+, 3'-UMP2-	His 12⁰, 3'-UMP2-
	Phosphate–Enzyme/Water Interactions		
O1P	His 12(N^{ε2}) His 12(N^{ε2})	His 12(N^{ε2}) His 119(N^{δ1}) Phe 120(N)	His 119(N^{δ1})
O2P	1 water		2 water
	Gln 11(N^{ε2})	His 12(N^{ε2})	Lys 7 (N^ζ) Gln 11(N^{ε2})
O3P	2 water	3 water	2 water
	His 119(N^{δ1})	His 119(N^{δ1}) 3 water	4 water
O3'		1 water	1 water
total	3 enzyme 3 water [3]	5 enzyme 7 water [5]	3 enzyme 9 water [6]
	Ribose–Enzyme/Water Interactions		
O2'	Lys 41(N^ζ)	Lys 41(N^ζ) (O2P)	Lys 41(N^ζ) (O2P)
	(O3')	(O3') 1 water	(O3')
total	1 enzyme 0 water [0]	1 enzyme 1 water [1]	1 enzyme 0 water [0]
	Base–Enzyme/Water Interactions		
O2	Thr 45(N)	Thr 45(N)	Thr 45(N)
N3	Thr 45(O^{γ1})	Thr 45(O^{γ1})	Thr 45(O^{γ1})
O4		1 water	
total	2 enzyme 0 water [0]	2 enzyme 1 water [1]	2 enzyme 0 water [0]
	Mononucleotide–Enzyme/Water Interactions		
total	6 enzyme 3 water [3]	8 enzyme 9 water [7]	6 enzyme 9 water [6]

[a] Numbers in square brackets indicate number of water *molecules* participating in hydrogen bonding, which may be less than or equal to the number of hydrogen bonds.

corresponding to protonated His 12 and 119 interacting with a dianionic phosphate, although there is not necessarily a direct correspondence between the number of interactions and the free energy of binding (see section V). At low pH there is a loss of 2 product–enzyme and 6 product–solvent interactions, whereas at neutral pH there is a loss of 2 product–enzyme interactions but no loss of product–solvent contacts. For both the optimal and neutral pH states where the phosphate is dianionic, the total number of solvent hydrogen bonds is the same (9), but it is less than that (3) for the low pH state where the phosphate is monoanionic. This implies that dianions in the active site are better solvated by water than monoanions.

A. Phosphate Interactions. Table 5 shows that in the optimal pH structure (pH = 5.5), the positively charged active site histidine residues both interact with *two* phosphoryl oxygens. This is consistent with their higher pK_a values upon nucleotide binding relative to the values in the free enzyme (see Table 1).[19] In addition, Phe 120(N) interacts with O1P, and Gln 11 is close to O2P (averaged distance = 3.62 Å) and may be bonding during part of the simulation. In the low pH structure, each of the two positively charged active site histidine residues interacts with only one phosphoryl oxygen, and the Phe 120–O1P hydrogen bond is lost. The reduced charge on the phosphate also results in a loss of four solvent–phosphate interactions. In the neutral pH structure, the enzyme–phosphate contacts are between protonated His 119(N^{δ1})–O1P, Gln 11(N^{ε2})–O2P, and Lys 7–O2P, which appears to compensate for the missing His 12(N^{ε2})–O2P interaction when His 12 is deprotonated. The lost interactions with the enzyme relative to the optimal binding state are partially compensated by two additional phosphate interactions with solvent; the increase in the number of phosphate–solvent bonds with pH correlates with the increase in the number of solvent molecules interacting with the phosphate, although some waters

(19) Blackburn, P.; Moore, S. *The Enzymes* **1982**, *15*, 317.

Table 6. 3'-UMP Product Interactions with Enzyme and Solvent as a Function of pH Using Atom-Switch and Atom-Shift Truncation Schemes[a]

	atom-switch			atom-shift	
	His 12+ 3'-UMP-	His 12+ 3'-UMP2-	His 12° 3'-UMP2-	His 12+ CpA-[b]	His 12° CpA-[c]
	Phosphate–Enzyme/Water Interactions				
O^{1P}	His 12($N^{\epsilon2}$)	His 12($N^{\epsilon2}$)			
		His 119($N^{\delta1}$)	His 119($N^{\delta1}$)	His 119($N^{\delta1}$)	His 119($N^{\delta1}$)
	Phe 120(N)	Phe 120(N)	Phe 120(N)	Phe 120(N)	Phe 120(N)
			2 water		
O^{2P}		His 12($N^{\epsilon2}$)		His 12($N^{\epsilon2}$)	
	5 water	3 water	3 water	2 water	2 water
O^{8P}	His 119($N^{\delta1}$)	His 119($N^{\delta1}$)			His 119($N^{\delta1}$)
	1 water	3 water	6 water		1 water
$O^{3'}$	1 water	2 water	3 water	1 water	
total	3 enzyme	5 enzyme	2 enzyme	3 enzyme	3 enzyme
	7 water [6]	8 water [5½]	14 water [6]	3 water	3 water
	Ribose–Enzyme/Water Interactions				
$O^{2'}$	His 12($N^{\epsilon2}$)		His 12($N^{\epsilon2}$)		His 12($N^{\epsilon2}$)
			Lys 41(N^{ζ})		Lys 41(N^{ζ})
		(O^{2P})	(O^{2P})		
				Phe 120(O)	
	($O^{3'}$)	($O^{3'}$)[d]	($O^{3'}$)[d]		
$O^{4'}$	1 water		1 water		
$O^{5'}$	1 water		1 water		
total	1 enzyme	0 enzyme	2 enzyme	1 enzyme	2 enzyme
	2 water [2]	1 water [½]	3 water [3]		
	Base–Enzyme/Water Interactions				
O^{2}	Thr 45(N)	Thr 45(N)	Thr 45(N)	Thr 45(N)	Thr 45(N)
N^{3}	Thr 45($O^{\gamma1}$)		Thr 45($O^{\gamma1}$)	Thr 45($O^{\gamma1}$)	Thr 45($O^{\gamma1}$)
				Thr 45(N)	
O^{4}		Ser 123(O^{γ})	Ser 123(O^{γ})		
	1 water	1 water	1 water	0 water	1 water
total	2 enzyme	2 enzyme	3 enzyme	3 enzyme	2 enzyme
	1 water [1]	1 water [1]	1 water [1]	0 water	1 water
	Mononucleotide–Enzyme/Water Interactions				
total	6 enzyme	7 enzyme	7 enzyme	7 enzyme	7 enzyme
	10 water [9]	10 water [7]	18 water [10]	3 water	4 water

[a] Numbers in square brackets indicate number of water *molecules* participating in hydrogen bonding, which may be less than or equal to the number of hydrogen bonds. [b] Reference 2. [c] Reference 16. [d] $H^{2'}$ acts as donor in hydrogen bond to solvent.

form two hydrogen bonds. Thus, at low and neutral pH, relative to the optimum pH, the electrostatic interactions between the enzyme and the phosphate group are reduced; at low pH this is due to the presence of the monoanion, and at neutral pH it is due to the deprotonation of His 12.

B. Ribose Interactions. In all X-ray structures of RNase A complexes, Lys 41 is disordered since it is very mobile; consequently, its role in catalysis or binding has been ambiguous. It is thus interesting that the extended electrostatic results show Lys 41(N^{ζ}) hydrogen bonding to $O^{2'}$ in all three protonation states. This suggests that Lys 41 plays an important role in binding the product, as well as in catalysis.[16] In the low and optimal pH states, the averaged conformation of the sugar is $C^{2'}$-exo, whereas it is $C^{2'}$-endo with slight $C^{3'}$-endo character at neutral pH (see Table 7).

Intramolecular hydrogen bonds are formed between $H^{2'}$ and $O^{3'}$ in the averaged structures at every pH, forming a five-membered "ring", $H^{2'}$–$O^{3'}$–$C^{3'}$–$C^{2'}$–$O^{2'}$–$H^{2'}$. There is also a hydrogen bond between $H^{2'}$ and O^{2P} in the optimal and neutral pH structures, forming an additional four-membered "ring", $H^{2'}$–O^{2P}–P–$O^{3'}$–$H^{2'}$ (see Table 5). The intramolecular contacts for the low pH structure are consistent with the X-ray structure where the five-membered ring is present but the $H^{2'}$–O^{2P} contact is missing. The latter is found only in the average molecular dynamics structures of the RNase A/3'-UMP complex having a dianionic phosphate.

C. Base Recognition. At all pH values, the uracil base has two interactions with Thr 45; in addition, there is one interaction (O^{4}) with a water molecule at the optimal pH. Similarly, the average molecular dynamics structures of RNase A/CpA complexes[2,16] show that the cytosine base interacts with Thr 45

at low and neutral pH where His 12 is protonated and neutral, respectively, and there is an additional solvent interaction with O^{4} at neutral pH (see Table 6). The presence of hydrogen bonds from the base to Thr 45 at all three pH values is consistent with the fact that Thr 45 is invariant in ribonucleases of 38 mammalian species.[20] The conformation of the base is anti for all three protonation states. It appears that the base conformation is not perturbed by binding to the enzyme since proton NMR studies[21] of 3'-CMP in D_2O solution at pD 5.2 and 7.2 indicate that the anti conformation is the low-energy conformation of 3'-CMP.

The aromatic ring of the Phe 120 residue is positioned such that solvent is excluded from the face of the base when the product is bound. In the crystal structure, the plane of the ring of Phe 120 is in an orientation between quasi-perpendicular and quasi-stacking with the plane of the base. In the simulations, the low pH structure had a quasi-perpendicular arrangement, while the optimal and neutral pH states remained in a configuration similar to the crystal structure.

D. Monoanionic Substrate vs Dianionic Product Interactions. A molecular dynamics simulation has been performed[2] on the solvated active site of RNase A complexed with the substrate, CpA, based on the low pH (pH = 5.5) crystal structure of RNase A/deoxy-CpA complex (see the last two columns of Table 6). This simulation was performed with the electrostatic shift option based on a cutoff distance of 8.5 Å. The interactions between the monoanionic phosphate, ribose, and cytidine base of CpA and the enzyme and solvent are very similar to those found for

(20) Beintema, J. J.; Lenstra, J. A. In *Macromolecules Sequences in Systematic and Evolutionary Biology*; Plenum: New York, 1982.
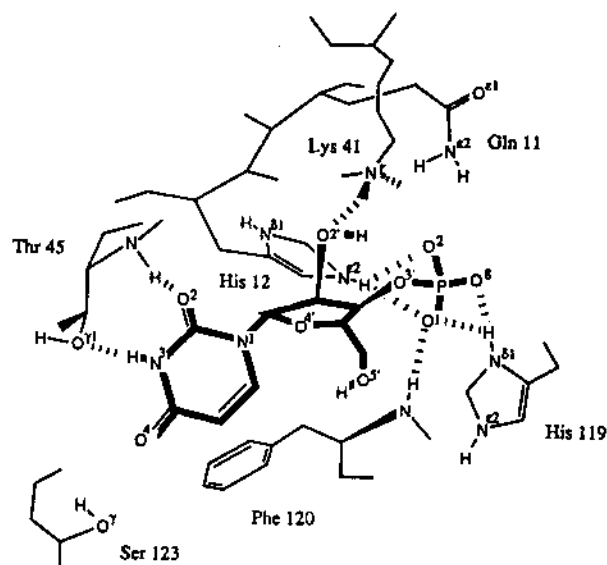
(21) Lavallee, D. K.; Coulter, C. L. *J. Am. Chem. Soc.* **1973**, *95*, 576.
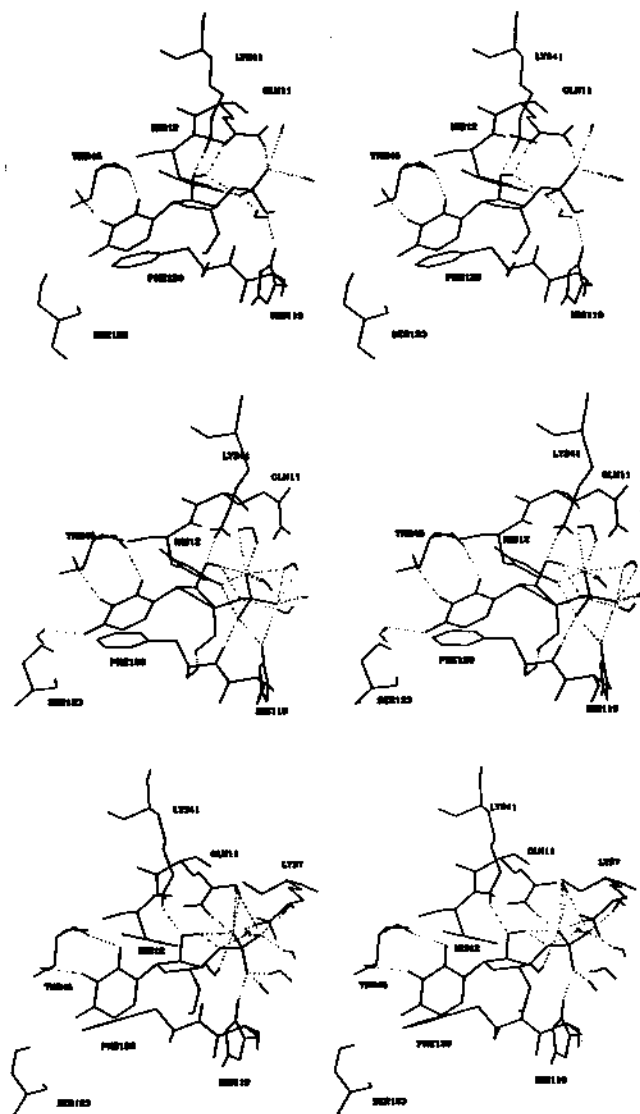
Figure 2. Stick representation of the RNase A/3'-UMP enzyme–product complex showing important hydrogen bonds between the product and residues of the enzyme active site as well as solvent molecules for (a, top) low pH with His 12⁺/3'-UMP⁻, (b, middle) optimal pH with His 12⁺/ 3'-UMP²⁻, and (c, bottom) neutral pH with His 12⁰/3'-UMP²⁻.

Figure 3. Schematic diagram of important hydrogen-bonding contacts between the key residues of the enzyme active site and the dianionic product (bold lines) in the average molecular dynamics structure at the pH of optimal binding.

Table 7. Base and Sugar Conformation in 3'-UMP

	His 12⁺, 3'-UMP⁻			His 12⁺, 3'-UMP²⁻			His 12⁰ 3'-UMP²⁻	
	X-ray	ASW[b]	EE[c]	ASW[b]	EE[c]	ASW[b]	EE[c]
				Base Conformation				
χ	−157.3 anti	−162.1 anti	−165.1 anti	−175.4 anti	−176.5 anti	−154.4 anti	−141.0 anti
				Sugar Conformation				
ν_0	9.50	10.64	3.99	3.67	18.85	8.17	−14.33
ν_1	−24.97	−21.30	−5.81	−25.34	−26.86	−24.97	2.06
ν_2	29.63	23.70	5.43	35.67	24.05	31.14	9.59
ν_3	−24.31	−17.39	−3.20	−33.31	−13.08	−27.02	−18.74
ν_4	10.00	4.35	−0.51	19.00	−3.68	12.21	21.14
$C^{2'}$	exo	exo	(exo)[a]	exo	exo	exo	endo
$C^{3'}$	endo	endo		endo		endo	endo

the low pH enzyme–product complex (Tables 5 and 6). Both complexes have the active site histidines protonated and the phosphate singly charged. Thus the binding of the substrate CpA to RNase A at pH 5.5 corresponds to the binding of the product 3'-UMP to RNase A at low pH (2–4). As a corollary, the simulation results suggest that the binding of the *monoanionic* substrate CpA to RNase A at pH 5.5 is weaker than the binding of the *dianionic* product 3'-UMP to RNase A at the same pH. The binding of the monoanionic substrate CpA to RNase A with His 12 neutral is also expected to be weaker than the binding of the dianionic product 3'-UMP to RNase A at pH 5.5, since the latter has an additional substrate–enzyme and five more substrate–solvent contacts than the former (Tables 5 and 6). This is in accord with the fact that the measured binding constants of monoanionic substrates are lower than those of corresponding dianionic products.[1]

In analogy to the results for RNase A/3'-UMP at low pH, the reduced charge on the phosphate monoanion of CpA relative to the dianion (3'-UMP²⁻) causes a loss of two phosphate interactions with protonated His 12 and 119, as well as a loss of phosphate–solvent interactions. Also, the total number of solvent hydrogen bonds for the monoanionic substrate is similar to that for the monoanionic product and is less than that for the dianionic product,

suggesting that monoanions are less well solvated compared to dianions in the active site.

E. Comparison of Extended Electrostatics with Atom-Switch Truncation. The results obtained with the atom-switch method for the enzyme–product interactions are similar to those obtained with the extended electrostatics model. However, there are a number of important differences that we consider below. For the water interactions, the behavior is very different in the two simulations. The number of product–solvent interactions is overestimated, particularly at low and neutral pH, compared to the extended electrostatics results, e.g., the total number of product–solvent interactions is 10 and 18 at low and neutral pH, respectively, compared to 3 and 9 predicted by extended electrostatics. The atom-switch truncation scheme also does not differentiate between the solvation of monoanionic and dianionic species since the number of product–solvent interactions at low and optimal pH is predicted to be equal, in contrast to the extended electrostatics results. The total number of product–enzyme and product–solvent interactions predicted by atom-switch truncation increases as a function of pH and is maximal for the neutral pH state of the RNase A/3'-UMP complex (Table 6), i.e., the number of enzyme (solvent) interactions is 6 (10), 7 (10), and 7 (18). At low pH, the total number of product–enzyme contacts predicted by the two methods is the same. This is probably due to the fact

that the electric field at a given distance from the phosphorus atom is weaker since the phosphate is singly charged at low pH.

With regard to phosphate–enzyme interactions, the atom-switch results do show some trend for the low, optimal, and neutral pH binding states, as in the extended electrostatics results. The interactions between the two active site histidines and the phosphate for all three protonation states are the same; this is also true of the Phe 120–phosphate interaction at optimal pH (Tables 5 and 6). However, the interactions between Phe 120 and O^{1P} at low and neutral pH (Table 6) are replaced by Gln 11–O^{2P} hydrogen bonds when the extended electrostatics method is employed (Table 6). In particular, the optimal binding state has five enzyme hydrogen bonds compared with three at low and two at neutral pH. The number of phosphate–solvent bonds increases monotonically with pH, but unlike the extended electrostatic results, the number of solvent molecules interacting with the phosphate is nearly constant $(6, 5^1/_2, 6)$ at all pH. (Here, $^1/_2$ indicates that the solvent molecule is hydrogen bonding to two sites of the protein or product.)
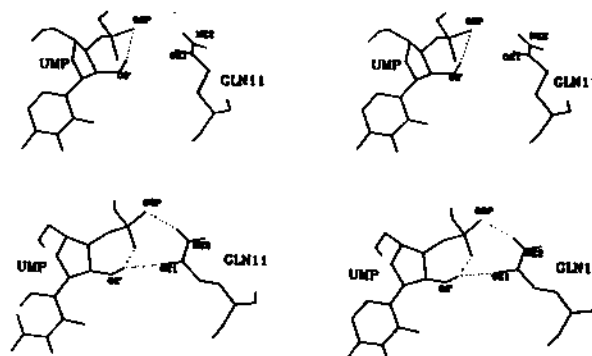
In contrast to the extended electrostatic results where Lys 41-(N^ζ) hydrogen bonds to $O^{2'}$ in all three protonation states, the atom-switch results for the low and optimal pH states indicate that Lys 41(N^ζ) does not interact with $O^{2'}$ even though the starting structures employed in the two methods were the same. Furthermore, for the low and neutral pH states, there are ribose–His 12 and ribose–solvent interactions which are absent in the extended electrostatics results. In contrast to the extended electrostatic results, where Lys 41 binds to the ribose independent of pH, Lys 41 binds to the ribose only for the neutral pH state with His 12 neutral. The intramolecular hydrogen bonds between $H^{2'}$ and $O^{3'}/O^{2P}$ found with extended electrostatics are maintained in the atom-switch results, as shown in Table 6.

As in the extended electrostatic results, Thr 45 is involved in binding to the base for all three protonation states. The atom-switch results predict that Ser 123 contributes to tighter binding of the base for the optimal and neutral pH states, while no bonding of Ser 123 to the base is seen in the extended electrostatics results. Using either extended electrostatics or atom-switch, the optimal pH state has two enzyme–base interactions. In contrast to the extended electrostatic results, the atom-switch results predict that O^4 interacts with a water molecule for the low pH state and with a water molecule and Ser 123 (O^γ) for the neutral pH state; these interactions are absent in the extended electrostatics results. The results for the atom-switch cutoff show that the low, optimal, and neutral pH states have a quasi-stacking arrangement of the Phe 120 and base. This is consistent with the $C^{3'}$-endo conformation of the ribose ring but does not follow the correlation with the χ angle of the base observed for the extended electrostatics results.

From the above comparison of the results obtained with the extended electrostatics and the atom-switch truncation method, it appears that strong, rigid interactions with well-positioned residues (His 12 and/or His 119 with the phosphate and Thr 45 with the base) are insensitive to the electrostatic model employed but that weaker interactions with solvent or Lys 41, which has greater flexibility, are more sensitive to details of the long-range forces.

IV. Concluding Discussion

Molecular dynamics simulations of the RNase/3'-UMP system using various truncation schemes have revealed several important features. Through an analysis of the average structures for three protonation states, a picture of the changing binding interactions in the enzyme–product complex emerges. To observe this it was found necessary to use the extended electrostatics method, which includes the full interactions of the system. A maximal number of binding interactions are found for dianionic phosphate interacting with both positively charged His 12 and His 119. This is in accord with the experimental result that strongest binding


Figure 4. Stick representation of the RNase A/3'-UMP enzyme–product complex isolating the conformations of Gln 11 (a, top) hydrogen bonding to the product in the extended electrostatics calculations and (b, bottom) failing to form hydrogen bonds to the product in the atom-switch simulations.

occurs for this system (see Tables 1 and 2). The fall in binding at low and neutral pH corresponds to the loss of enzyme interactions with the phosphate and base observed in the simulation. This is of particular interest because an X-ray structure is available only for the low pH state, and in that structure, very few water molecules are observed in the binding site,[2] presumably because there is considerable disorder. It is shown, not surprisingly, that monoanions are less well solvated than dianions in the active site. The loss of monoanionic phosphate–solvent interactions at low pH may contribute to the decrease in binding. A positively charged active site histidine (His 12 or His 119), Lys 41, and Thr 45 are involved in phosphate, ribose, and base recognition, respectively, for the three protonation states considered. Thus, all the groups of the product are involved in binding. Specific interactions involving polar and charged groups play an essential role at the different pH values. X-ray data in these pH ranges would be of interest to test the predictions. The results are consistent with the observation that the interaction of nucleosides is stronger than that of either ribose or free base and that nucleotides are more strongly bound than nucleosides.[1] The binding also involves Phe 120, which interacts with the phosphate.

An interesting correlation concerns the orientation of the side chain of Gln 11 (see Figure 4). In the crystal structure, the χ_1 side-chain dihedral angle $(N–C^\alpha–C^\beta–C^\gamma)$ is $-53.18°$, which corresponds to the carbonyl group pointing toward the phosphate and the hydrogen bond-donating $N^{\epsilon 2}$ pointing away. In all of the calculations employing the extended electrostatics, there is a dihedral angle transition for the χ_1 angle of Gln 11, and at the low and neutral pH states (and nearly so at optimal pH), there is a change in χ_1 leading to the formation of a hydrogen bond between the phosphate and $N^{\epsilon 2}$ of Gln 11. For the atom-switch calculations, there is no dihedral angle transition in Gln 11 and no formation of a hydrogen bond to the phosphate at any pH. It appears likely that the crystal structure has interchanged the $O^{\epsilon 1}$ and $N^{\epsilon 2}$ atoms.

The atom-switch truncation scheme leads to results which disagree with the experimentally observed binding as a function pH. It predicts an increase in the number of product–enzyme as well as the total number of product–solvent interactions with increasing pH. Thus maximal binding would be expected to occur for the neutral pH state instead of the observed pH 5.5. Further, the atom-switch truncation scheme does not yield the correct charge dependence of solvation since the number of phosphate–solvent interactions is similar for both monoanionic (low pH) and dianionic (optimal pH) phosphate but differs significantly at maximal and neutral pH, where the phosphate is in the same charged state. Another key difference between atom-switch versus extended electrostatics results is that for the optimal binding state at pH 5.5, the former show no enzyme contacts with the ribose, whereas the latter show that the Lys 41 is involved in

2598 *J. Am. Chem. Soc., Vol. 116, No. 6, 1994*

Straub et al.
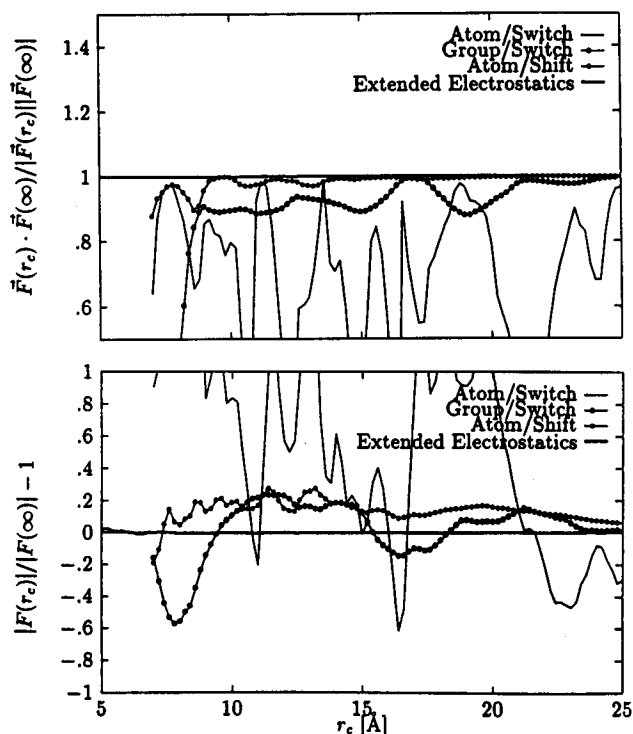
Figure 5. Force on the phosphorus atom interacting with all atoms within a cutoff distance, r_c, as a function of the cutoff distance for group-switch, atom-switch, and atom-shift truncation, and the extended electrostatics method.

binding the sugar. Although the strong polar interactions, particularly with rigid groups, tend to be insensitive to the electrostatic model, a number of the enzyme–product and the product–solvent interactions are significantly different.

Even if the cutoff distance included the entire active site region, atom truncation with shift or switch should be used with care. We find that an accurate treatment of the RNase A/3'-UMP system requires inclusion of all charges in the system and their long-range electrostatic forces. Although this can be accomplished by using no potential cutoff, the computational requirements are prohibitive. We have shown in this example that the extended electrostatic method, where the electrostatic forces outside a transition charge distance are approximated by a multipole expansion up to the quadrupole term, provides an accurate estimate of the long-range forces with manageable computational requirements even for systems composed of several thousand atoms. In light of the present results, we conclude that the extended electrostatics method is preferred over other truncation schemes in systems where electrostatic interactions are expected to be dominant.

Appendix

In this section we present a limited truncation error analysis by comparing the direction and magnitude of the forces acting on the product phosphate P and O^{2P} atoms as a function of the cutoff distance r_c for four truncation schemes.
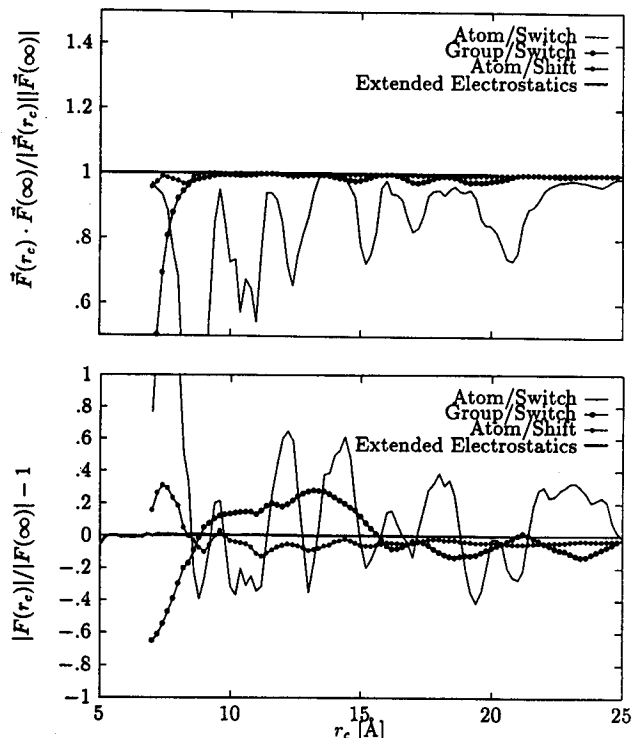
Figure 6. Force on the phosphoryl oxygen, O2P, interacting with all atoms within a cutoff distance, r_c, as a function of the cutoff distance for group-switch, atom-switch, and atom-shift truncation, and the extended electrostatics method.

Figure 5 shows the magnitude and direction of the relative force on the phosphorus atom interacting with all atoms (enzyme and solvent) within a cutoff distance as a function of the cutoff distance for the various truncation schemes used; the corresponding plot for one of the phosphoryl oxygens, O^{2P}, is given in Figure 6. The crystal structure and a 4-Å switching region was employed. Using group-switch with a cutoff distance of 13 Å, the magnitude and direction of the forces on the phosphorus atom and O^{2P} are within 10% of the corresponding no-cutoff forces. In contrast, using atom shift

$$S(r) = \begin{cases} [1 - 2(r/r_c)^2 + (r/r_c)^4] & r \leq r_c \\ 0 & r > r_c \end{cases} \quad (7)$$

with a cutoff distance of $r_c = 12$ Å, the magnitude of the O^{2P} force does not converge to the no-cutoff value even at a cutoff distance of 25 Å. Similarly, using atom-switch with a cutoff distance of 13 Å, the magnitude and direction of the forces on the phosphorus atom and O^{2P} exhibit oscillatory behavior and do not converge until the cutoff distance is greater than 25 Å. Thus, with cutoffs ≤ 12 Å, the greater stability of the enzyme–inhibitor complex using atom-switch truncation compared to group-switch is unexpected since the latter truncation scheme yields forces which are closer to the no-cutoff forces relative to the atom truncation schemes.

Since the forces calculated with the various truncation schemes do not converge until the cutoff distance is at least 25 Å, long-range electrostatic interactions between the phosphate group and the enzyme are present, possibly involving the positively charged surface lysine residues, and contribute to the stability of the enzyme–inhibitor complex. The extended electrostatics method takes into account the electrostatic interactions between all atom pairs in an approximate manner so that with a cutoff of 12 Å, the force is closest to the exact (no-cutoff) force.

Loncharich and Brooks[22] performed a detailed investigation of the effects of truncating long-range forces in simulations of

(22) Loncharich, R. J.; Brooks, B. R. *Proteins* **1989**, *6*, 32.

carboxymyoglobin. Our analysis is in agreement with their conclusion that a long-range atom shift ($r_c \geq 12$ Å) is recommended over a group-switch or atom-switch truncation. However, from a limited analysis of forces on atoms as a function of cutoff (Figures 5 and 6), it is difficult to see why the group-switch truncation fails to provide as accurate an estimate of the magnitude and direction of the force for a cutoff of 12 Å or why the atom-switch truncation leads to a stable bound conformation. One might speculate that the atom-switch truncation scheme results in a "comb potential" which has the tendency to lock the system into restricted conformations reducing the atomic fluctuations.

A related result has recently been presented by Smith and Pettitt[23] in a simulation comparison of the atom-switch, group-switch, and Ewald summation schemes for treating the electro-static potential of a peptide in ionic solution. Their results corroborate our conclusions and those of Loncharich and Brooks[22] who found that the atom-switch truncation results in reduced flexibility and smaller atomic fluctuations compared with the group-switch truncation or Ewald summation method. As Smith and Pettitt emphasize, a consequence of artifacts arising from the truncation method is that the simulation results can become very sensitive to the choice of initial conditions.

(23) Smith, P. E.; Pettitt, B. M. *J. Chem. Phys.* **1991**, *95*, 8430.
(24) Tanokura, M. *J. Biochem.* **1983**, *94*, 1621.
(25) Haar, W.; Maurer, W.; Ruterjans, H. *Eur. J. Biochem.* **1974**, *44*, 201.
(26) Markley, J. L. *Biochemistry* **1975**, *14*, 3546.
(27) Andersen, H. C.; Hammes, G. G.; Walz, F. G. *Biochemistry* **1968**, *7*, 1637.
(28) Weiner, S. J.; Kollman, P. A.; Case, D. A.; Singh, U. C.; Ghio, C.; Alagona, G., Jr.; Profeta, S.; Weiner, P. *J. Am. Chem. Soc.* **1984**, *106*, 765.